8177

NACA

RESEARCH MEMORANDUM

THRUST AND DRAG CHARACTERISTICS OF A CONVERGENT-DIVERGENT NOZZLE WITH VARIOUS EXHAUST JET TEMPERATURES

By Donald P. Hearth and Fred A. Wilcox

Lewis Flight Propulsion Laboratory
Cleveland, Ohio

NATIONAL ADVISORY COMMITTEE
FOR AERONAUTICS

WASHINGTON
March 11, 1954

[redacted]

NATIONAL ADVISORY COMMITTEE FOR AERONAUTICS

RESEARCH MEMORANDUM

THRUST AND DRAG CHARACTERISTICS OF A CONVERGENT-DIVERGENT NOZZLE WITH VARIOUS EXHAUST JET TEMPERATURES

By Donald P. Hearth and Fred A. Wilcox

SUMMARY

An investigation was conducted in the 8- by 6-foot supersonic wind tunnel on the effect of exhaust-gas temperatures on the external and internal characteristics of a convergent-divergent nozzle having an area expansion ratio of 1.83. Data were obtained over a pressure-ratio range from 1 to 20 at free-stream Mach numbers of 1.6 and 2.0 for exhaust temperatures of 860°, 1650°, and 2000° R.

Results of this investigation indicated that generally both the internal and external performance characteristics were only slightly affected by a large change in jet temperature. The small differences in performance which did occur were predicted satisfactorily from theoretical considerations.

INTRODUCTION

The experimental evaluation of exhaust-nozzle performance (refs. 1 to 3, for example) have usually been made at relatively low exhaust jet temperatures. In order to apply the results of such investigations to full-scale engines, a knowledge of the difference in nozzle performance, if any, due to higher jet temperatures is required. Numerous investigations, such as reference 4, have been conducted on the internal characteristics of rocket-engine nozzles utilizing high jet temperatures. Although the effect of jet temperature and continued burning within a convergent-divergent nozzle has been treated analytically in reference 5, no experimental evaluation of this problem has been made, and a comparison between cold jet nozzle flow and hot jet flow is not available.

The internal and external performance of several exhaust-nozzle configurations installed on a generalized jet exit model has been obtained in the NACA 8- by 6-foot supersonic wind tunnel (refs. 1 and 2).

[redacted]

[redacted]

Investigated as a part of this program was a convergent-divergent nozzle having an area expansion ratio of 1.83. The thrust characteristics of this nozzle with a cold jet (860° R) are included in reference 1. This same nozzle was also investigated at jet temperatures of 1650° and 2000° R, achieved by inserting a combustor prior to the nozzle. At these temperatures, data were obtained at free-stream Mach numbers of 1.6 and 2.0 and for pressure ratios up to 20. The results of the investigation are presented herein and compared with the cold jet nozzle performance.

SYMBOLS

The following symbols are used in this report:

A	area, sq ft
C_D	drag coefficient, $\frac{D}{q_0 A_m}$
C_P	pressure coefficient, $\frac{p - p_0}{q_0}$
D	drag force, lb
F	jet thrust, $m_i V_2 + A_2(p_2 - p_0)$, lb
F_i	ideal jet thrust, $m_i V_{2_i}$, lb
F/F_i	jet thrust ratio
q	dynamic pressure, $\frac{\gamma p M^2}{2}$, lb/sq ft
M	Mach number
P	total pressure, lb/sq ft
P_1/p_0	nozzle pressure ratio
p	static pressure, lb/sq ft
R	radius, ft
T	total temperature, °R

V	velocity, ft/sec
γ	ratio of specific heats
ρ	static density, slugs/cu ft

Subscripts:

a	boattail
b	base
i	ideal
m	maximum
0	free stream
1	nozzle entrance
2	nozzle exit
*	nozzle throat

APPARATUS AND PROCEDURE

The exit model on which the nozzle was investigated was installed in the 8- by 6-foot supersonic wind tunnel as shown in figure 1. Air flow was measured with an A.S.M.E. sharp-edge orifice and the internal model pressure was varied with a throttle valve located downstream of the orifice. The air was preheated to a temperature of 860° R by a coventional turbojet can combustor prior to entering the model.

The preheated air was then introduced into the model through the two hollow support struts as indicated in figure 1. The desired exhaust temperatures were obtained by means of the combustor shown in figure 2 as it was installed in the model. This main burner consisted of a combustor dome attached to a conical basket having holes totaling 110 percent of the combustion-chamber cross-sectional area. Unleaded gasoline was used and ignition was obtained with a turbojet-engine spark plug mounted in the dome. Approximately half of the fuel was injected in an axial direction through a variable-orifice nozzle in the dome and the rest inward at an angle of 45° through four fixed-area nozzles 5 inches downstream of the dome. Fuel flow to both the main burner and the preheater was measured with rotameters.

As shown in figure 2, the model consisted of an inner liner within which the internal air flow was confined and an outer shell. The outer shell had a parabolic nose section 40 inches long (eq. shown on fig. 2) and a cylindrical section (outside diam., $8\frac{1}{4}$ in.) 34.13 inches long. The exhaust-nozzle configuration investigated consisted of a nozzle located inside a parabolic boattail (fig. 2). Pressure instrumentation and internal nozzle coordinates are shown in figure 3. The nozzle was of the convergent-divergent type having a throat area of 0.090 square feet and an expansion ratio of 1.83. This area ratio corresponded to a design pressure ratio (one-dimensional flow) of 9.1 and 8.1 for γ of 1.40 and 1.30, respectively.

Jet thrust was obtained in the same manner as discussed in detail in reference 1. The increment of jet thrust in the diverging nozzle section was obtained from an integration of the static wall pressures in this section, and the result added to the computed thrust of a sonic nozzle. The jet thrust thus obtained neglected any losses occurring in the convergent portion and any friction losses occurring in the divergent portion of the nozzle. Internal performance of the nozzle is presented in terms of a jet thrust ratio, the ratio of actual jet thrust to ideal jet thrust. Ideal jet thrust for any one pressure ratio is defined as that thrust available from a given throat area nozzle if the nozzle expanded isentropically to free-stream static pressure. It should be noted that the thrust ratio is based on actual and ideal thrusts for a nozzle mass flow coefficient of 1.0. In the actual case this coefficient was not unity but rather 0.99. The additional refinement of correcting the thrust ratio for nozzle flow coefficient does not significantly affect its value.

Drag characteristics were evaluated in the same manner discussed in reference 2. The jet effects on the integrated boattail pressure drag and on the pressure in the base region (fig. 3) were determined.

The jet temperature was calculated at the nozzle throat from continuity relationships. For this computation the nozzle mass flow coefficient was assumed equal to the cold flow value (0.99), and the total pressure at the nozzle throat was assumed equal to the total pressure at the nozzle entrance. The hot data fell generally into two ranges: $1650^\circ \pm 100^\circ$ R and $2000^\circ \pm 100^\circ$ R. In addition, data were obtained at 860° R with the main burner installed.

DISCUSSION

External Characteristics

The effect of a hot jet issuing from the nozzle on the boattail pressure drag is presented in figure 4 for free-stream Mach numbers

of 1.6 and 2.0 and jet temperatures of 860°, 1650°, and 2000° R. Integration of boattail pressure distributions was used to obtain the drag values shown. Within the data scatter, the boattail drag variation with nozzle pressure ratio appears to have been essentially the same for jet temperatures up to 2000° R.

Influence of the hot jet on the base pressure is indicated in figure 5. Although changing the jet temperature did not affect the trend of base pressure coefficient $C_{P,b}$ with nozzle pressure ratio, at any given pressure ratio higher base pressure coefficients resulted from higher jet temperatures, thus reducing the base drag.

A method of estimating base pressures with a hot jet from cold jet data is discussed in reference 6. The assumption is made that the nozzle pressure ratio which produces the same base pressures for various values of γ (representing a change in jet temperature) also yields the same Prandtl-Meyer expansion angle. A curve of the base pressure coefficient determined from the cold data ($\gamma = 1.40$) and adjusted by the method of reference 6 to $\gamma = 1.30$ (which corresponds to an exhaust temperature of approximately 2000° R) is included in figure 5. Comparison between the 2000° R data and the estimated curve indicates fairly good agrement. This agreement may be coincidental, and additional verification at higher jet temperatures and with other nozzle configurations is obviously needed to prove the applicability of the correlation method.

Schlieren photographs of the cold ($T_* = 860°$ R) and a hot ($T_* = 2000°$ R) jet at a free-stream Mach number of 2.0 are presented in figure 6. (It should be noted that the dark horizontal strip near the center of the jet is the upper half of the wake from the horizontal model support struts.) The movement upstream of the trailing shock for an increase in nozzle pressure ratio appears to have been slightly greater for the hot case (note figs. 6(c) and 6(f)). This small difference in shock movement did not significantly affect boattail drag as shown in figure 4.

Internal Characteristics

Pressure distributions in the diverging portion of the nozzle are presented in figures 7 and 8 for exhaust temperatures of 2000° and 1650° R, respectively. Included on these figures are the distributions (no internal shocks) for the same nozzle with an exhaust temperature of 860° R (ref. 1). As indicated, the operation of the nozzle with a hot jet of given temperature was similar to cold jet operation in that at higher values of pressure ratios ($P_1/p_0 > 8.6$) the static-pressure

distributions within the nozzle were independent of a change in both nozzle pressure ratio and free-stream Mach number. Jet temperature does, however, influence the absolute values of the nozzle local static pressures. Raising the jet temperature resulted in an increase in the local static pressures. For example, at an area ratio A_x/A_* of 1.30 the local pressure ratios p_x/P_1 were 0.159, 0.170, and 0.178 for jet temperatures of 860°, 1650°, and 2000° R, respectively.

The theoretical pressure distributions for isentropic one-dimensional flow are included in figures 7 and 8 for a γ of 1.40. This value of γ corresponds approximately to a jet temperature of 860° R. As noted in reference 1, the experimental pressure distributions fall substantially below the one-dimensional theory, no doubt because of nonuniform Mach number distributions across the nozzle. Better theoretical agreement with the cold data is shown in reference 1 with distributions based on the method of characteristics. As the exhaust temperature is increased, the ratio of specific heats γ decreases. Values of γ of 1.30 and 1.34 correspond approximately to jet temperatures of 2000° and 1650° R, respectively. For comparison with the distributions at $\gamma = 1.40$, the theoretical pressure distributions as calculated from isentropic one-dimensional flow for γ values of 1.30 and 1.34 are included in figures 7 and 8, respectively. It appears, therefore, that the higher static-pressure distributions obtained with the hot jets are due primarily to differences in γ.

Because the burner combustion efficiencies were low (approximately 50 percent) there is the possibility of some burning and heat addition in the nozzle. If such heat additions did occur, it also would cause a static-pressure increase in the diverging portion of the nozzle (see ref. 5). The amount of nozzle heat addition appears, however, to have been very small, for figures 7 and 8 indicate essentially the same difference between experimental pressures, with and without main burning, as the theoretically predicted difference assuming no burning in the nozzle.

The nozzle thrust characteristics are presented in terms of the ratio of actual jet thrust to ideal jet thrust. Actual jet thrust was obtained by the same pressure integration technique used in reference 1 and was refined to include the change in sonic thrust due to the different values of γ involved (1.30 for $T_* = 2000°$ R and 1.34 for $T_* = 1650°$ R). Ideal jet thrust was calculated for isentropic expansion from a sonic throat to free-stream static pressure. The ideal thrust parameter is presented in figure 9 for γ values of 1.30 and 1.40. It is apparent that the ideal thrust is slightly affected by γ.

The jet thrust ratios for exhaust temperatures of 2000° and 1650° R are presented in figure 10 and are compared with the cold jet results of reference 1. In the upper portions of figure 10 the ideal jet thrust is based on the same value of γ (1.40) for both the hot and cold case, while in the lower portion the ideal thrust is based on the γ corresponding to the actual jet temperature. The upper portion of this figure illustrates the slightly higher actual thrusts obtained with a hot jet than with the cold jet due primarily to the higher level of static pressures in the diverging section of the nozzle. On the other hand when the actual and ideal thrusts are both based on the appropriate γ (the lower portions of fig. 10) the true measure of the nozzle performance and the effect of jet temperature are apparent. Below a nozzle pressure ratio of approximately 10, slightly higher thrust ratios were obtained at the elevated jet temperatures, whereas above this pressure ratio greater thrust ratios were obtained with the cold jet.

This experimentally observed difference can be predicted from theoretical considerations. Presented in figure 11 are the theoretical one-dimensional thrust ratio characteristics at $\gamma = 1.30$ and 1.40. Calculations were made as in references 1 and 3 and are presented as the ratio of the jet thrust for isentropic one-dimensional expansion for a nozzle with an expansion ratio of 1.83 to the jet thrust for isentropic one-dimensional expansion to free-stream static pressure (fig. 9). It is interesting to note that as the gas properties change (different values of γ) the theoretical thrust ratio characteristics are different. Comparison of this figure with the lower portions of figure 10 indicates essentially the same theoretical difference in thrust ratio characteristics as was obtained experimentally.

SUMMARY OF RESULTS

The following results were obtained from an investigation conducted in the 8- by 6-foot supersonic wind tunnel on a convergent-divergent nozzle having an area expansion ratio of 1.83. Data were obtained at free-stream Mach numbers of 1.6 and 2.0 and jet temperatures of 860°, 1650°, and 2000° R.

1. The absolute value of boattail drag and its variation with nozzle pressure ratio were generally insensitive to the jet temperature.

2. Raising the jet temperature resulted in an increase in the coefficient of base pressure. For the configuration evaluated, it was possible to predict this change from cold jet data.

3. Higher static pressures in the divergent portion of the nozzle were noted as the exhaust temperature was raised and are believed due to the different expansion characteristics caused by the lower value of γ.

4. The thrust ratio is slightly influenced by jet temperature. Although the change in this ratio is not unidirectional with jet temperature, it can be theoretically predicted from one-dimensional considerations.

Lewis Flight Propulsion Laboratory
National Advisory Committee for Aeronautics
Cleveland, Ohio, December 29, 1953

REFERENCES

1. Fradenburgh, Evan A., Gorton, Gerald C., and Beke, Andrew: Thrust Characteristics of a Series of Convergent-Divergent Exhaust Nozzles at Subsonic and Supersonic Flight Speeds. NACA RM E53L23.

2. Hearth, Donald P., and Gorton, Gerald C.: Investigation of Thrust and Drag Characteristics of a Plug-Type Exhaust Nozzle. NACA RM E53L16.

3. Krull, H. George, and Steffen, Fred W.: Performance Characteristics of One Convergent and Three Convergent-Divergent Nozzles. NACA RM E52H12, 1952.

4. Foster, Charles R., and Cowles, Frederick B.: Experimental Study of Gas-Flow Separation in Overexpanded Exhaust Nozzle for Rocket Motors. Pro. Rep. No. 4-103, Jet Prop. Lab., C.I.T., May 9, 1949. Ordinance Dept. Contract No. W-04-200-ORD-455.

5. Hearth, Donald P., and Perchonok, Eugene: Analysis of Heat Addition in a Convergent-Divergent Nozzle. NACA TN 2938, 1953.

6. Cortright, Edgar M., Jr., and Kochendorfer, Fred D.: Jet Effects on Flow over Afterbodies in Supersonic Stream. NACA RM E53H25, 1953.

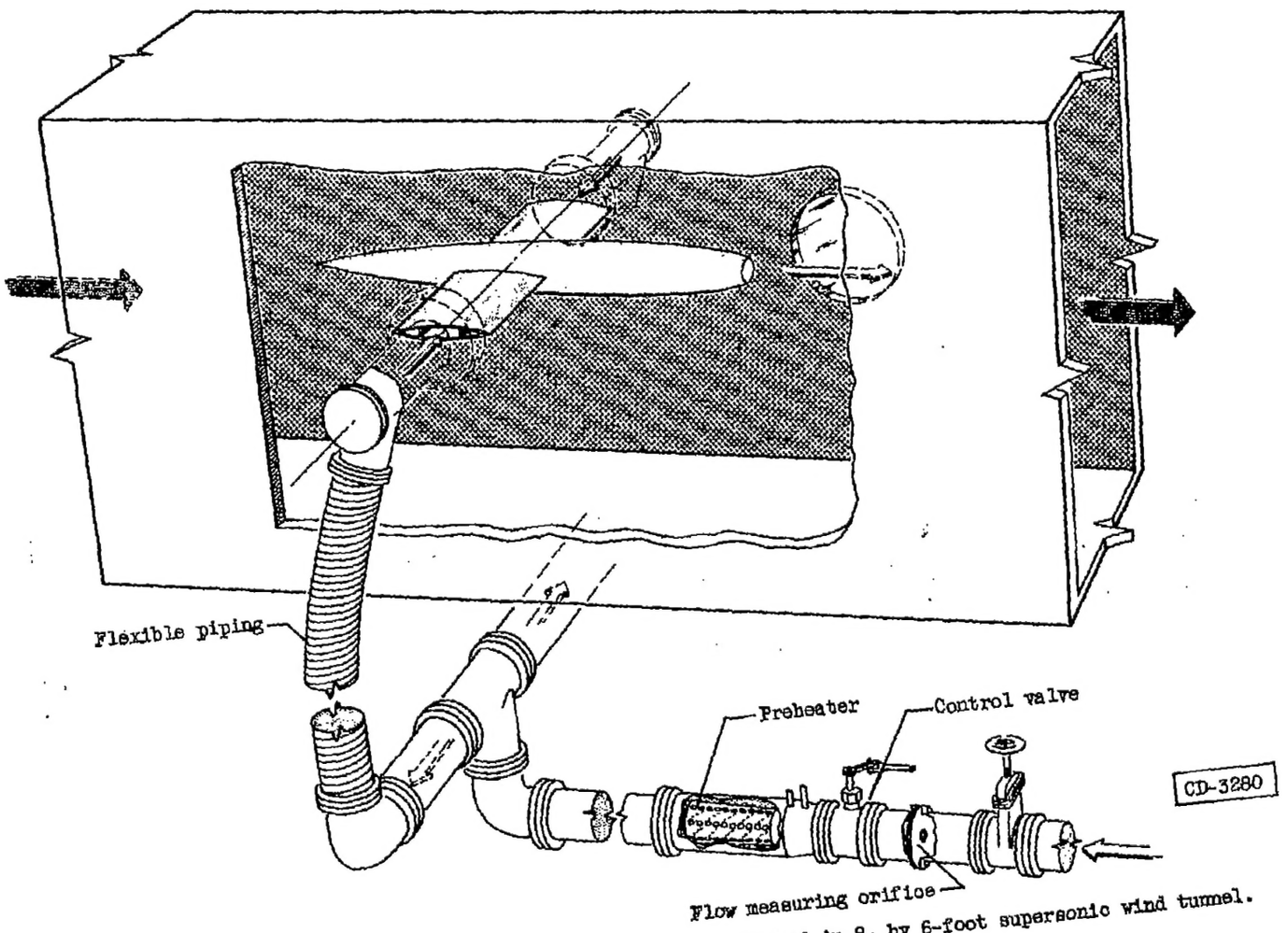

Figure 1. - Schematic drawing of jet exit model installed in 8- by 6-foot supersonic wind tunnel.

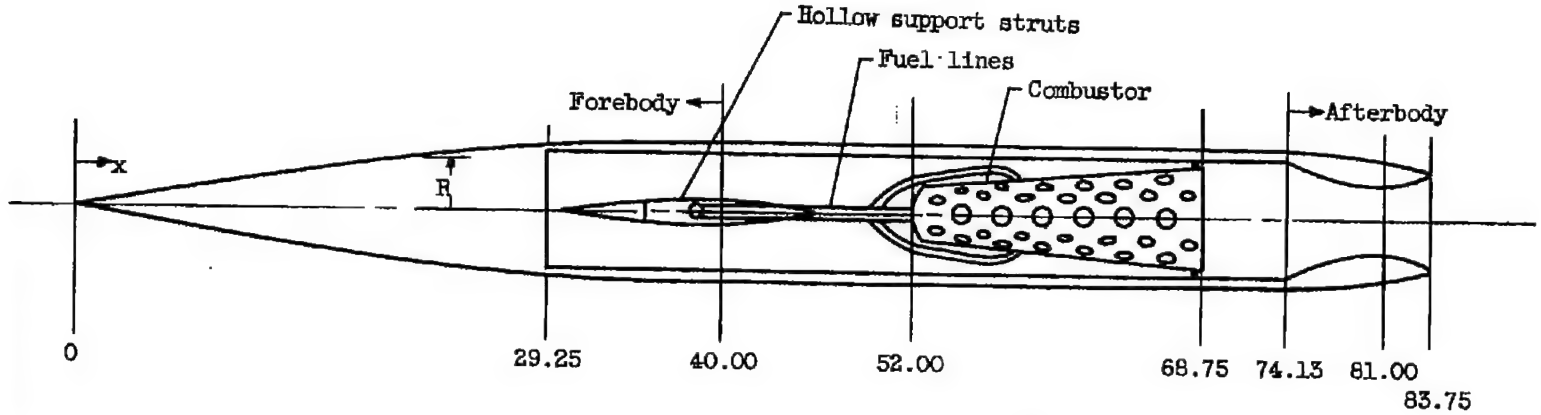

Equation of forebody contour: $R = 4\frac{1}{8}\left[1 - \left(\frac{40-x}{40}\right)^2\right]$

Equation of afterbody contour: $R = 4\frac{1}{8}\left[1 - \left(\frac{x-74.13}{18}\right)^2\right]$

Figure 2. - Jet exit model.

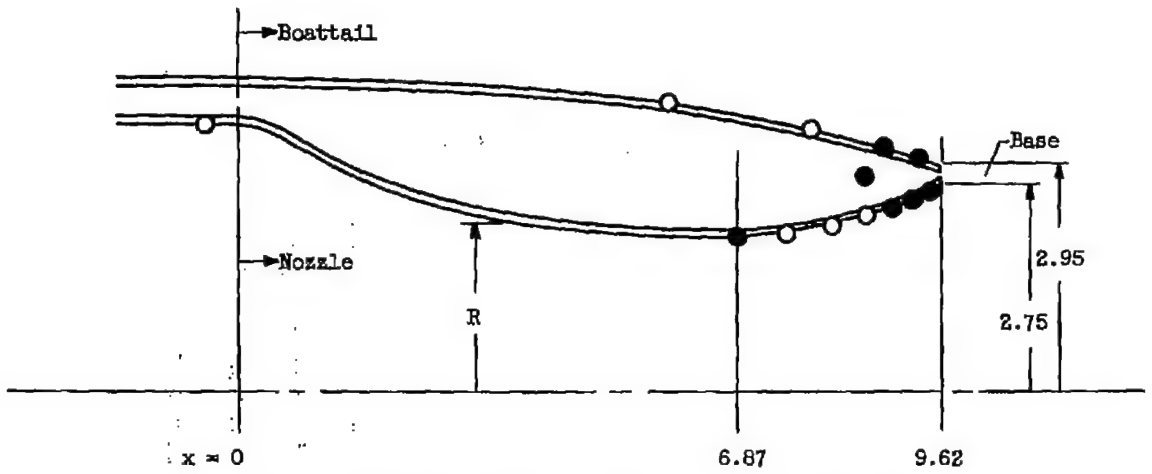

Convergent coordinates	
x	R
0	3.50
0.47	3.48
0.87	3.28
1.87	2.62
2.87	2.24
3.87	2.08
4.87	2.035
5.87	2.031
6.87	2.030

Divergent coordinates	
x	R
6.87	2.030
7.37	2.06
7.87	2.15
8.37	2.27
8.87	2.43
9.12	2.52
9.37	2.62
9.62	2.75

Figure 3. - Nozzle and boattail contours showing location of pressure instrumentation. (All dimensions are in inches.)

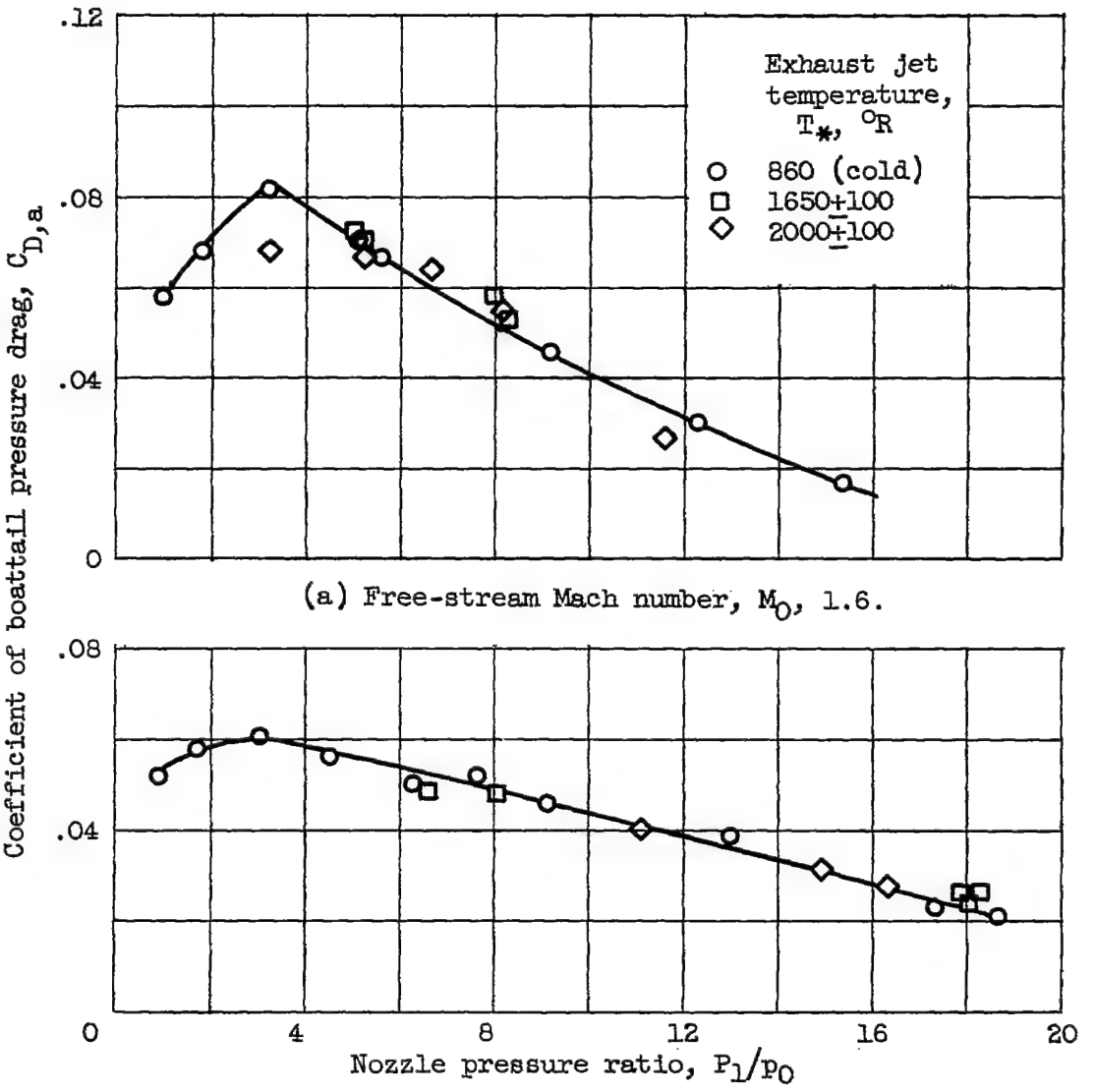

(a) Free-stream Mach number, M_0, 1.6.

(b) Free-stream Mach number, M_0, 2.0.

Figure 4. - Effect of jet temperature on boattail pressure-drag characteristics.

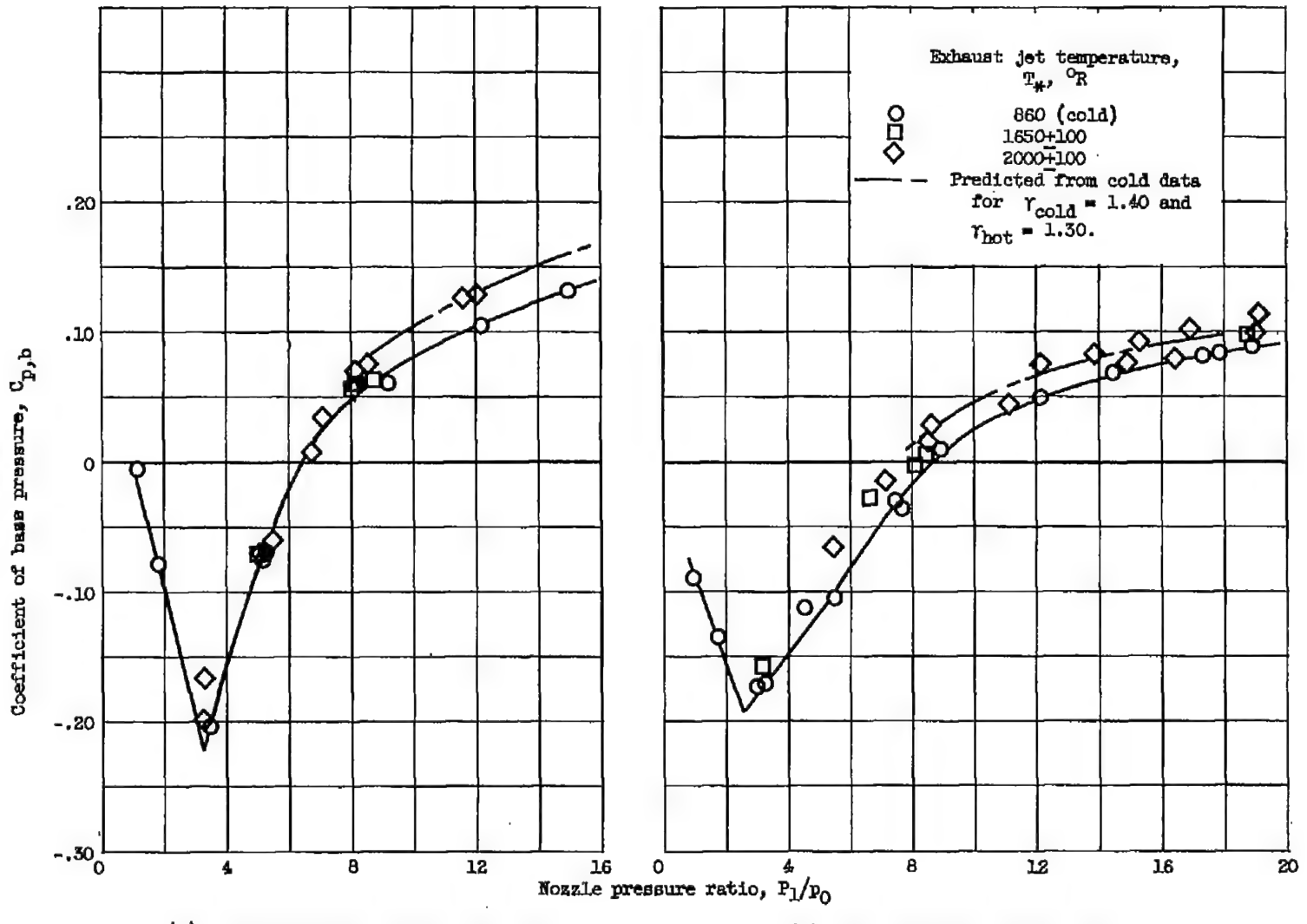

(a) Free-stream Mach number, M_0, 1.6.

(b) Free-stream Mach number, M_0, 2.0.

Figure 5. - Effect of jet temperature on base pressure characteristics.

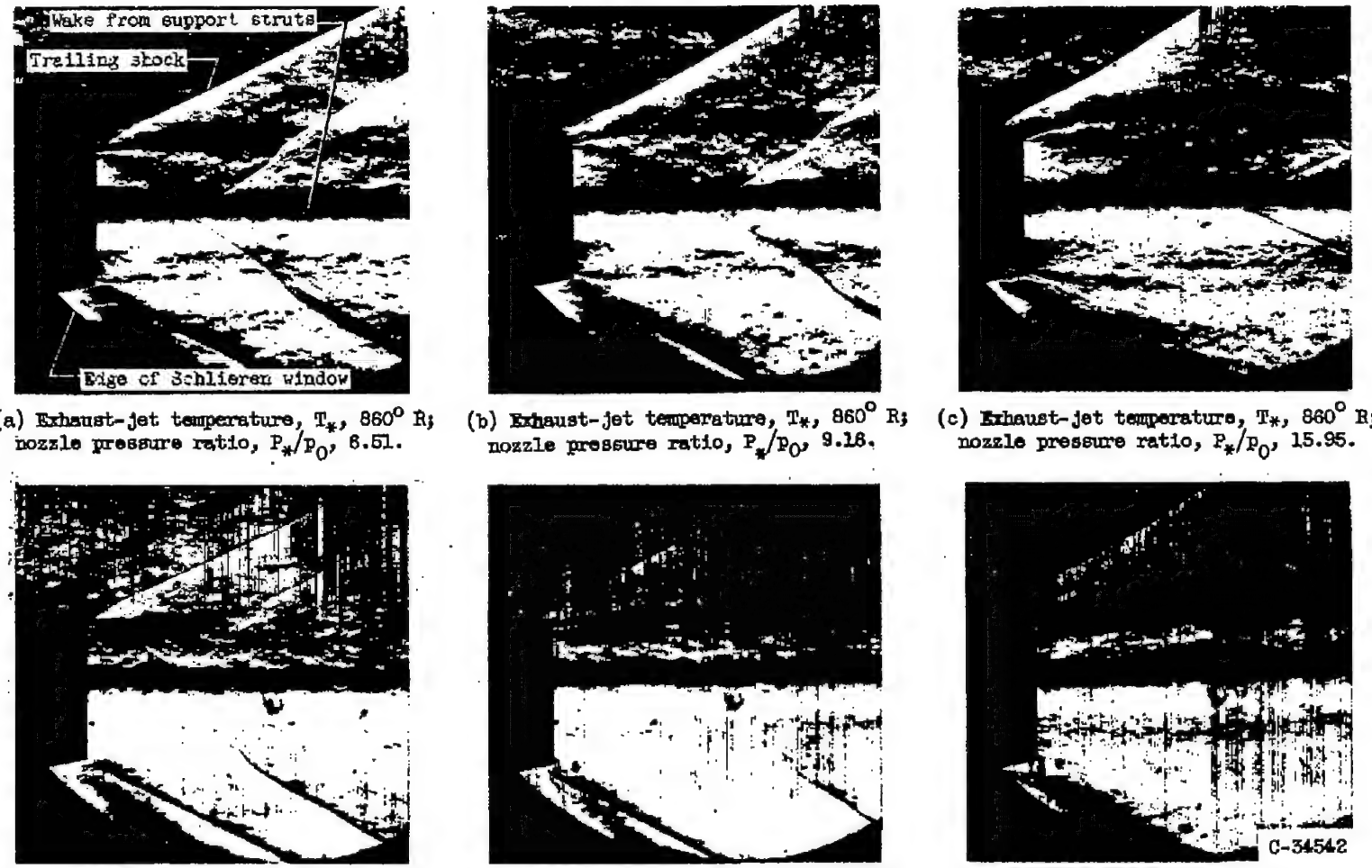

(a) Exhaust-jet temperature, T_*, 860° R; nozzle pressure ratio, P_*/p_0, 6.51.

(b) Exhaust-jet temperature, T_*, 860° R; nozzle pressure ratio, P_*/p_0, 9.18.

(c) Exhaust-jet temperature, T_*, 860° R; nozzle pressure ratio, P_*/p_0, 15.95.

(d) Exhaust-jet temperature, T_*, 2000° ± 100° R; nozzle pressure ratio, P_*/p_0, 5.36.

(e) Exhaust-jet temperature, T_*, 2000° ± 100° R; nozzle pressure ratio, P_*/p_0, 8.60.

(f) Exhaust-jet temperature, T_*, 2000° ± 100° R; nozzle pressure ratio, P_*/p_0, 15.33.

Figure 6.- Schlieren photographs of nozzle exit. Free-stream Mach number, M_0, 2.0.

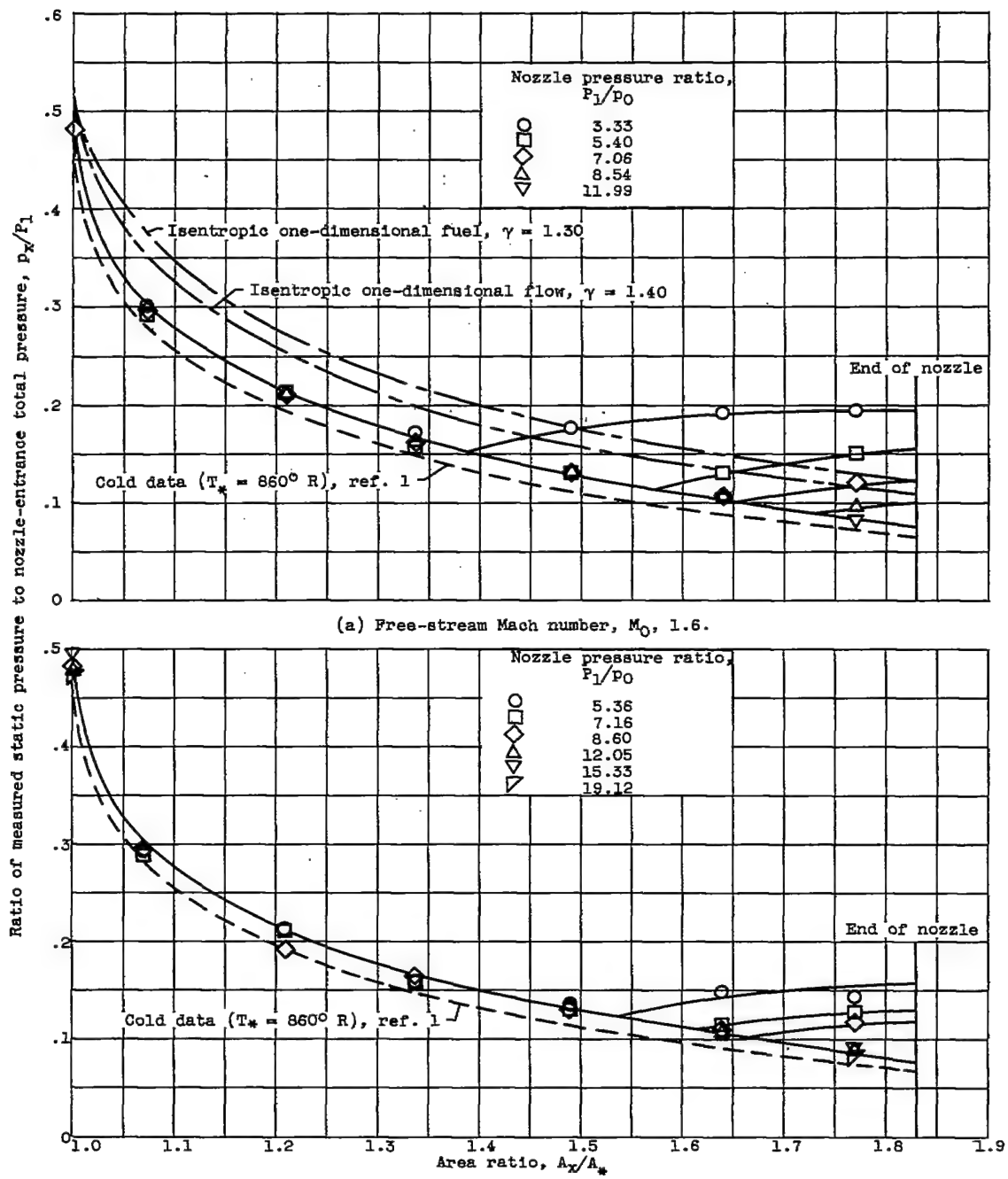

(a) Free-stream Mach number, M_0, 1.6.

(b) Free-stream Mach number, M_0, 2.0.

Figure 7. - Static-pressure distribution through diverging nozzle section for jet temperature of 2000°±100° R.

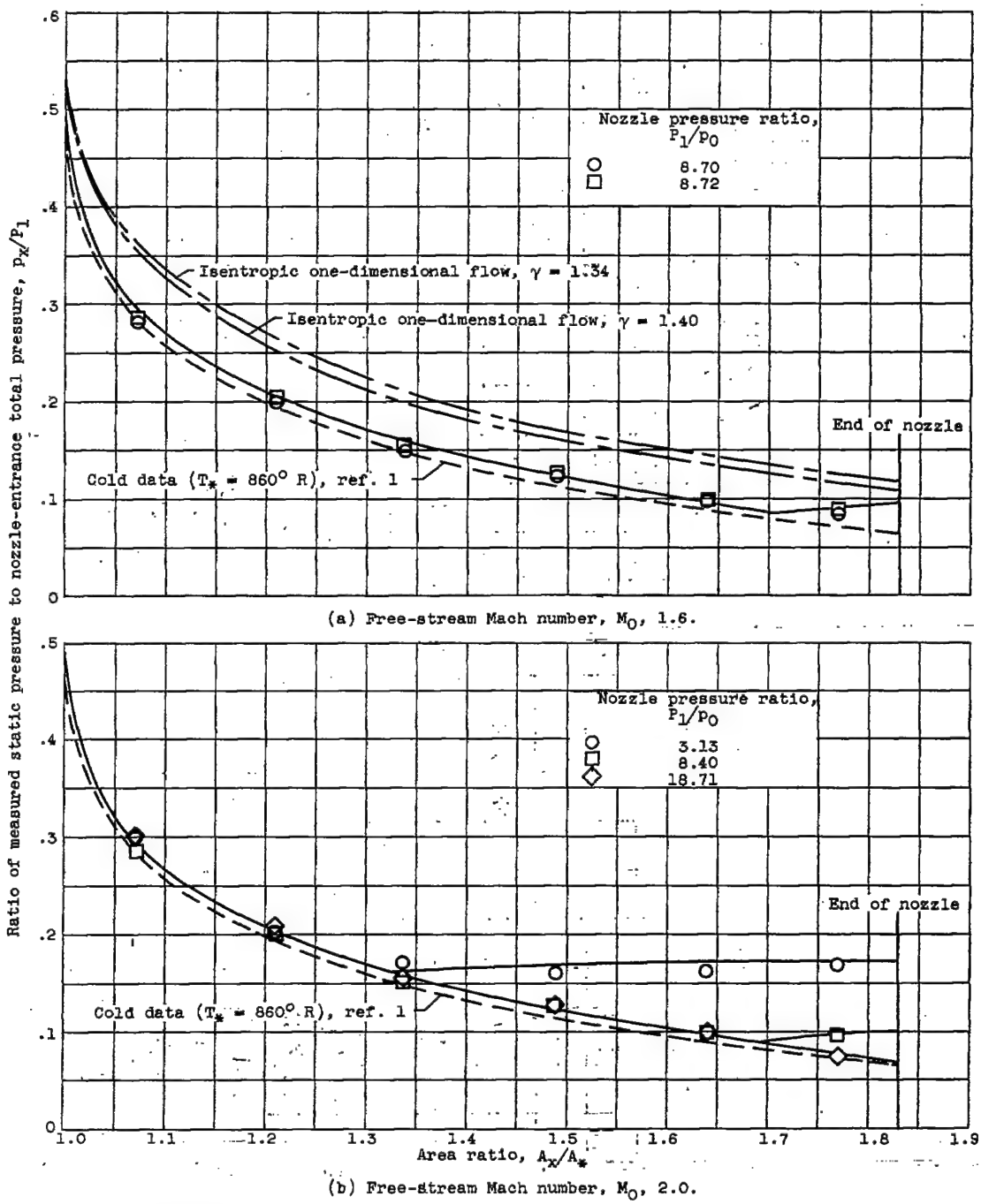

Figure 8. - Static-pressure distribution through diverging nozzle section for jet temperature of 1650°±100° R.

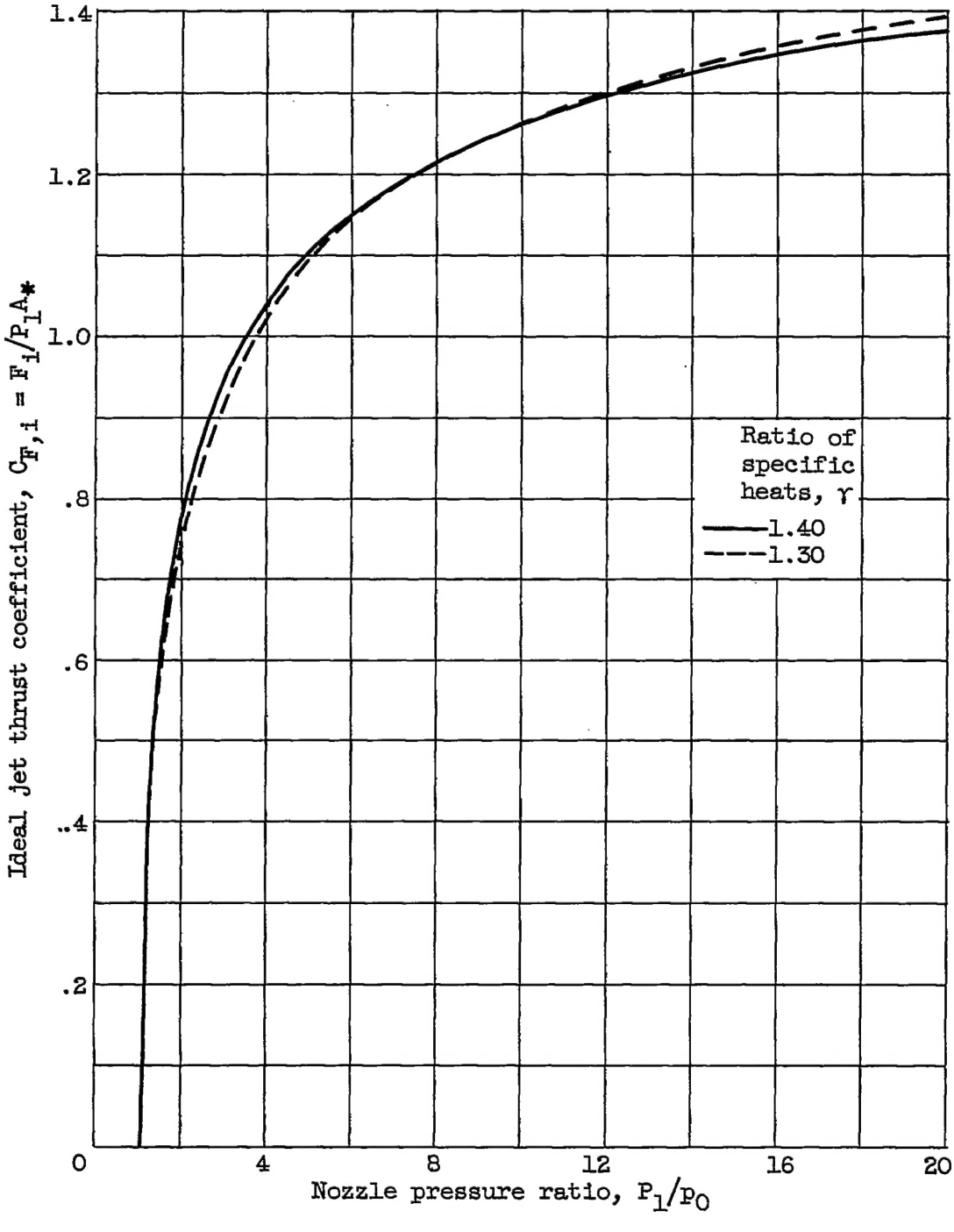

Figure 9. - Ideal jet thrust coefficient for isentropic expansion to free-stream static pressure.

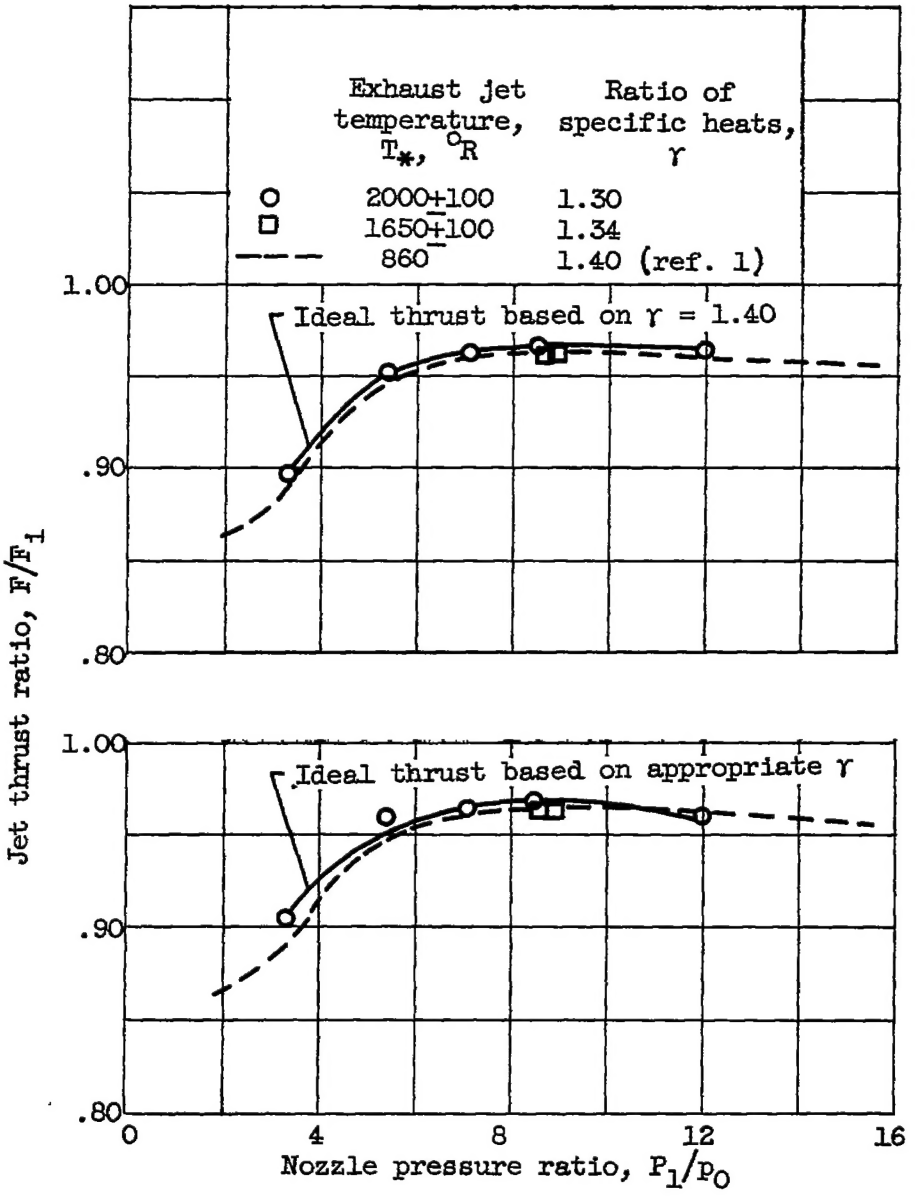

(a) Free-stream Mach number, M_0, 1.6.

Figure 10. - Effect of jet temperature on nozzle thrust characteristics.

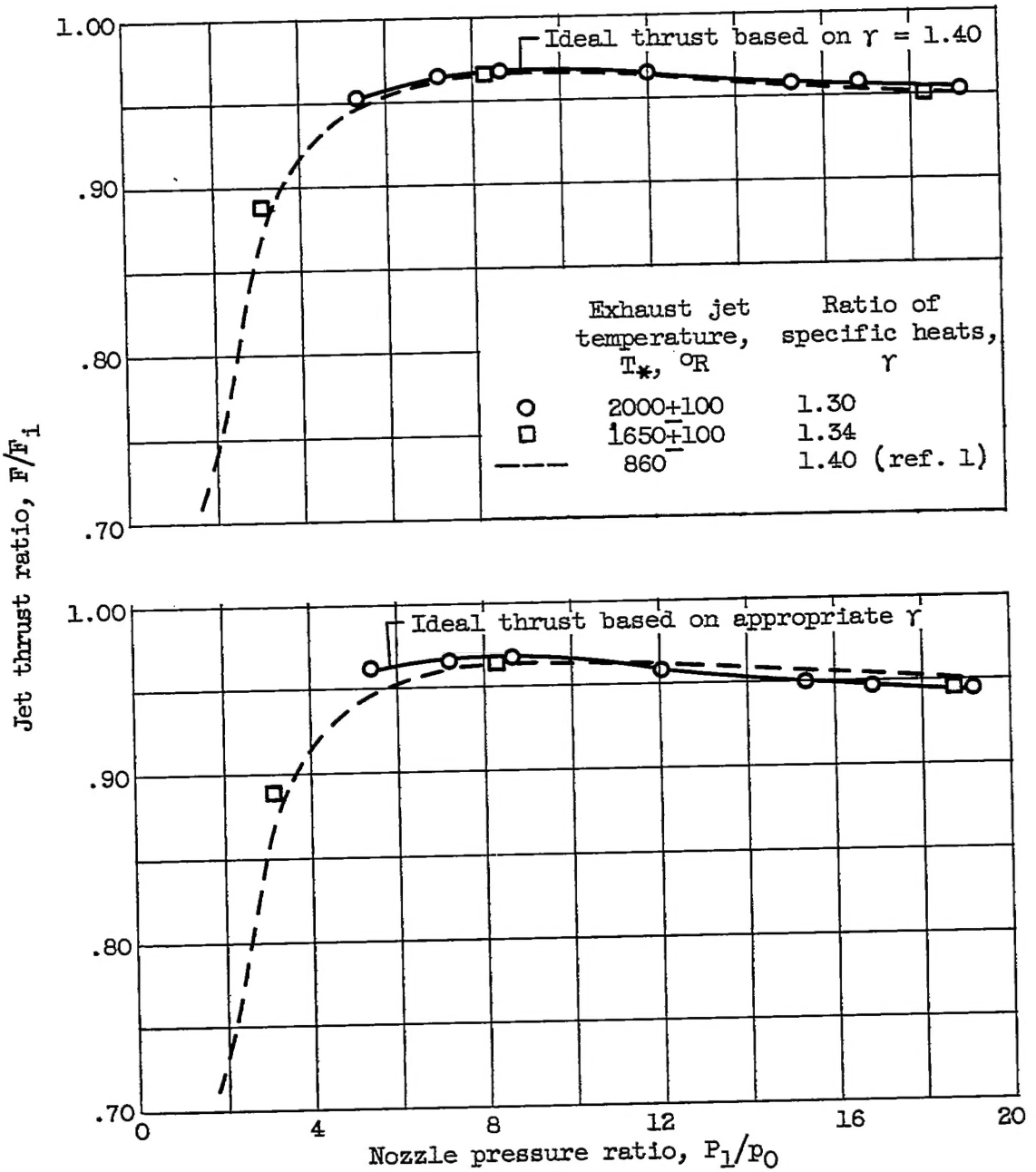

(b) Free-stream Mach number, M_0, 2.0.

Figure 10. - Concluded. Effect of jet temperature on nozzle thrust characteristics.

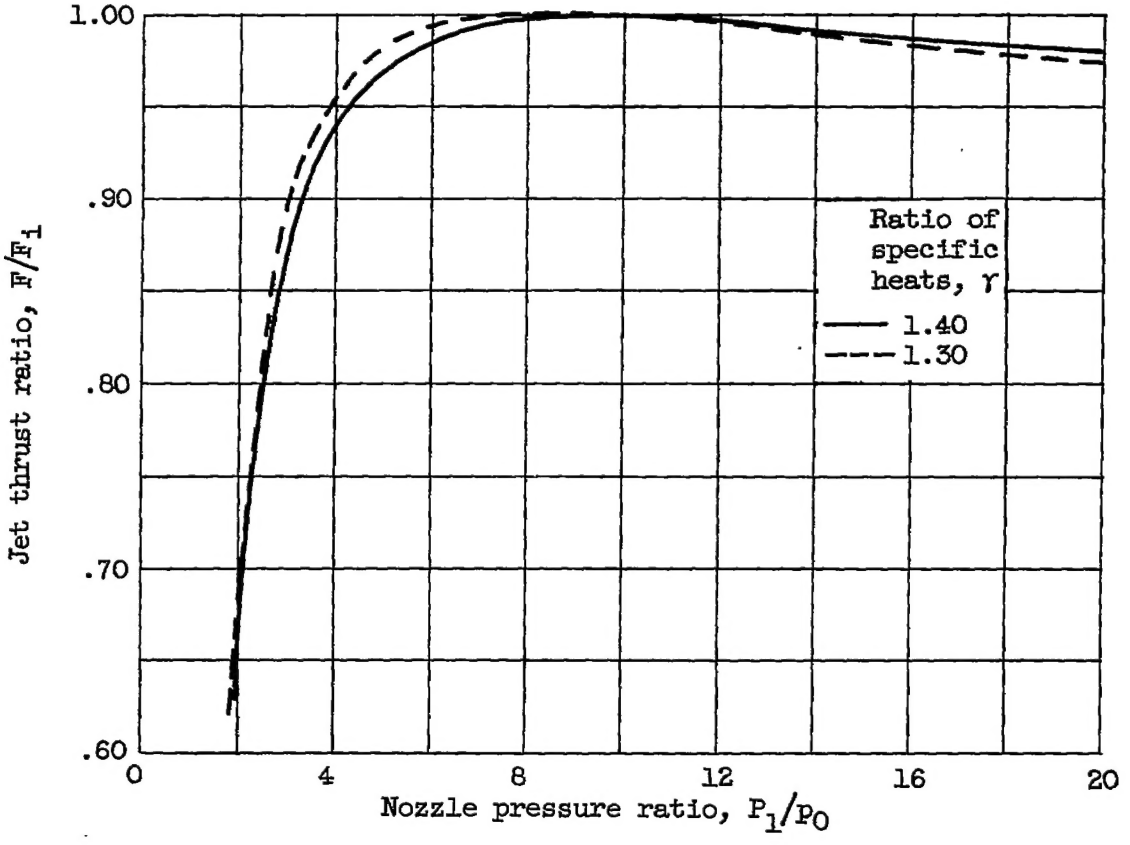

Figure 11. - Thrust ratio characteristics for nozzle with expansion ratio of 1.83 (one-dimensional theory).

NACA-Langley - 3-11-54 - 325